Hyperconnectivity and Slow Synapses during Early Development of Medial Prefrontal Cortex in a Mouse Model for Mental Retardation and Autism

Guilherme Testa-Silva[1], Alex Loebel[2], Michele Giugliano[3,4,5], Christiaan P.J. de Kock[1], Huibert D. Mansvelder[1] and Rhiannon M. Meredith[1]

[1]Department of Integrative Neurophysiology, Center for Neurogenomics and Cognitive Research, Neuroscience Campus Amsterdam, VU University, 1081 HV, Amsterdam, The Netherlands, [2]Department Biologie II, Ludwig-Maximilians University and Bernstein Center for Computational Neuroscience, D-82152 Munich, Germany, [3]Department of Biomedical Sciences, University of Antwerp, B-2610 Wilrijk, Belgium, [4]Laboratory of Neural Microcircuitry, Brain Mind Institute, EPFL, CH-1015 Lausanne, Switzerland and [5]Department of Computer Science, University of Sheffield, S1 4DP Sheffield, UK

Mansvelder and Meredith shared senior authorship

Address correspondence to Rhiannon M. Meredith, De Boelelaan 1085, 1081 HV, Amsterdam, The Netherlands. Email: rmered@falw.vu.nl.

Neuronal theories of neurodevelopmental disorders (NDDs) of autism and mental retardation propose that abnormal connectivity underlies deficits in attentional processing. We tested this theory by studying unitary synaptic connections between layer 5 pyramidal neurons within medial prefrontal cortex (mPFC) networks in the Fmr1-KO mouse model for mental retardation and autism. In line with predictions from neurocognitive theory, we found that neighboring pyramidal neurons were hyperconnected during a critical period in early mPFC development. Surprisingly, excitatory synaptic connections between Fmr1-KO pyramidal neurons were significantly slower and failed to recover from short-term depression as quickly as wild type (WT) synapses. By 4–5 weeks of mPFC development, connectivity rates were identical for both KO and WT pyramidal neurons and synapse dynamics changed from depressing to facilitating responses with similar properties in both groups. We propose that the early alteration in connectivity and synaptic recovery are tightly linked: using a network model, we show that slower synapses are essential to counterbalance hyperconnectivity in order to maintain a dynamic range of excitatory activity. However, the slow synaptic time constants induce decreased responsiveness to low-frequency stimulation, which may explain deficits in integration and early information processing in attentional neuronal networks in NDDs.

Keywords: autism, EPSC, Fragile X, hyperconnectivity, prefrontal cortex

Introduction

Development of cognitive function requires the formation and refinement of cortical neuronal networks. In neurodevelopmental disorders (NDDs) of autism and mental retardation, abnormal neuronal connectivity is proposed to underlie the cognitive and behavioral deficits (Belmonte et al. 2004; Geschwind and Levitt 2007). Impaired long-range synchronization and increased local connectivity is observed in **functional magnetic resonance imaging** studies in autism (Just et al. 2004; Dinstein et al. 2011). Abnormalities in dendrite and spine structure are found in both autistic human postmortem tissue and genetic NDD mouse models (Purpura 1974; Huttenlocher 1990; Chapleau et al. 2009). These findings point toward changes in functional synaptic connectivity (Belmonte and Bourgeron 2006; Geschwind and Levitt 2007).

Attentional deficits and impaired executive function are common to a range of autistic NDDs (Ewen and Shapiro 2005). The medial prefrontal cortex (mPFC) has specific roles in attention and executive function (Goldman-Rakic 1995; Miller 2000). Duration and timing of recurrent synaptic activity in prefrontal cortex are proposed to be key neural correlates underlying these behaviors (Miller et al. 1996; Gill et al. 2000; Fuster 2001). However, it is not known if abnormalities in temporal synaptic activity within mPFC occur in disorders of autism and retardation.

In this study, we used the Fmr1-KO genetic mouse model for Fragile X syndrome, one of the most common known genetic causes of mental retardation and autism (Silverman et al. 2010), to measure if changes in connectivity and synaptic dynamics occur in local networks of principal output neurons during mPFC development. We found significant hyperconnectivity between layer 5 pyramidal neurons in mPFC in Fmr1-KO mice, providing a functional correlate of the theories of abnormal connectivity in NDDs (Belmonte et al. 2004). These synapses exhibited significantly delayed recovery from short-term depression compared with wild types (WTs). Both abnormal connectivity and slow synapse recovery of Fmr1-KO synapses were restricted to 2–3 weeks postnatal development and returned to normal by 3–5 weeks age. To dissect the early consequences of hyperconnectivity and slowed temporal processing, we investigated their impact on the behavior of an excitatory cortical model network. In a hyperconnected "Fmr1-KO" network, delayed recovery from synaptic depression was crucial to enable a dynamic range of spontaneous activity across excitatory neurons. Nonetheless, stimulation of the Fmr1-KO network at an input-specific range of frequencies revealed impaired low-pass filtering properties of the network compared with the control network. Thus, slower temporal synaptic function is necessary to counterbalance hyperconnectivity, but as a result, may underlie the deficits in integration and processing of information during an early developmental stage of attentional networks in NDDs.

Materials and Methods

Animals

Male and female Fmr1-KO1 mice (Bakker et al. 1994) backcrossed on a Harlan C57BL/6 background strain for 10 generations were used with WT same strain C57BL/6 in all experiments. Mice ages ranged from P12 to 36 and were decapitated prior to slice preparation, in accordance with Dutch license procedures.

Slice Preparation and Storage

Brains were rapidly removed and dissected in ice-cold artificial cerebrospinal fluid (aCSF) containing the following in mM: 110

choline chloride; 11.6 sodium ascorbate; 7 MgCl$_2$; 3.1 Na-pyruvate; 2.5 KCl; 1.25 NaH$_2$PO$_4$; 0.5 mM CaCl$_2$; 26 NaHCO$_3$; 10 glucose (~300 mOsm).

Coronal slices of the prelimbic region of the mPFC were cut on a vibrating microtome at 300 μ (P12–19) and 450 μ (P20–36) thickness and then placed in a submerged-style holding chamber in aCSF, bubbled with carbogen (95% O$_2$, 5% CO$_2$) containing the following in mM: 126 NaCl; 3 KCl; 1 NaH$_2$PO$_4$; 1 MgSO$_4$; 2 CaCl$_2$; 26 NaHCO$_3$; 10 glucose. Slices were allowed to recover for 20 min at 33 °C followed by 40 min at room temperature.

Electrophysiology

Pyramidal cells were visualized in layer 5 of the prelimbic region of mPFC using infrared differential interference contrast microscopy and selected on the basis of morphology and basic cell firing pattern. Cell identity was reconfirmed by inclusion of biocytin (0.5%) to the intracellular pipette medium and processed immunohistochemically. The recorded cells were revealed with the chromogen 3,3′diamino-benzidine tetrahydrochloride (DAB) using the avidin–biotin–peroxidase method (Horikawa and Armstrong 1988)

Current-clamp recordings were made at 33 °C in a submerged-style chamber with patch pipettes (4–6 MOhm) pulled from borosilicate capillary glass and filled with an intracellular solution containing (in mM): potassium gluconate 135, 4-(2-hydroxyethyl)-1-piperazineetha-nesulfonic acid 10, phosphocreatine 10, MgATP 2, GTP 0.3, NaCl 4, EGTA 0,2 and 0.5% biocytin, which pH was adjusted at 7.3.

Clusters of 5–6 layer 5 pyramidal cells were stimulated and recorded using multiple whole-cell patch clamp. Direct synaptic connections were examined by eliciting short trains of precisely timed action potentials (APs) at 30 Hz followed by a recovery-test response 500 ms later (Fig. 1A Inset). Voltage recordings were amplified using Axoclamp-700B amplifiers (Axon instruments, Foster City, CA), filtered at 3 kHz and digitized at 5–20 kHz (ITC-1600; Instrutech, New York, NY) and acquired via scripts written for Igor Pro (Wavemetrics, Lake Oswego, OR).

Connectivity Indices and Statistical Analysis

Two to three clusters were obtained from each animal for only one slice. For cluster analysis, slices were viable for statistical analysis if post hoc staining revealed intact dendritic morphologies of all patched neurons and, in the absence of direct monosynaptic excitatory connections, an evoked, indirect inhibitory connection could be observed between at least 2 pyramidal neurons to demonstrate intact circuitry within the slice. The significance of differences among connection rates was determined using two-sided chi-square test and Wilcoxon sum rank test. The index used to quantify connectivity and to compare values along intersomatic distances, was:

The connection probability (CP), a measure of connection likelihood over all possible connections (assuming that they are independent events), defined as:

$$CP = \frac{N_C}{N_{PC}} \qquad (1)$$

where N_C stands for the total number of connections found and N_{PC} is the number of possible connections, which depends on the number of cells patched. By performing paired-recordings on a cluster of C cells, the number of possible connections between these cells is $N_{PC} = C \cdot (C-1)$, that is, the number of all possible combinations of monosynaptic connections between C cells.

The position of each cell patched was recorded in (x, y, z) coordinates, and the above indices are then calculated as function of the Euclidian distance.

All index data is presented as mean ± standard error of the mean (SEM), which was calculated assuming binomial data distribution by,
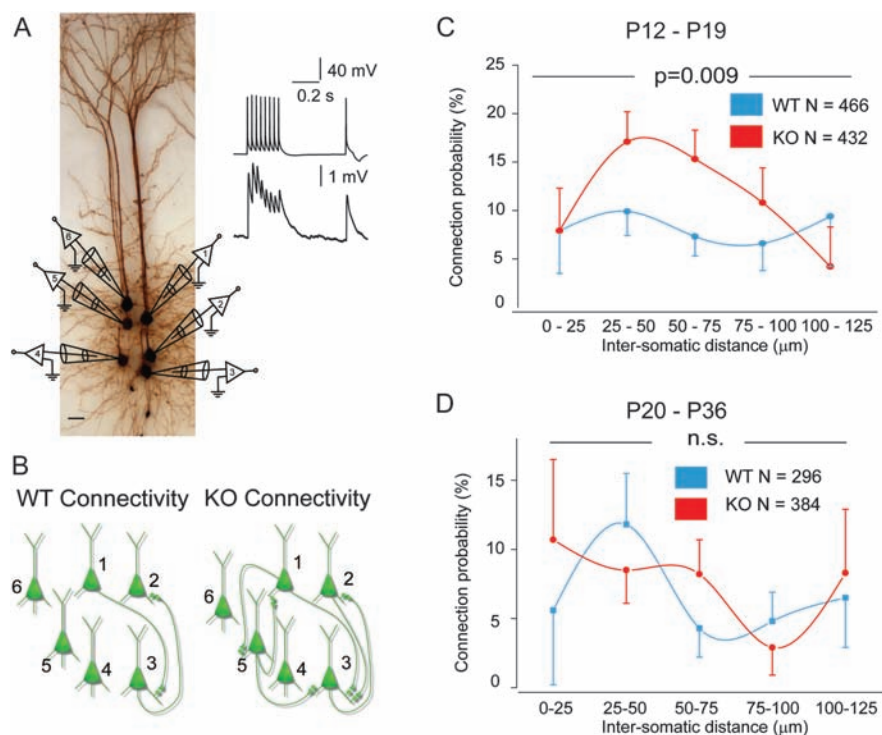
Figure 1. Hyperconnectivity of layer 5 pyramidal neurons in mPFC of 2–3 week but not 3- to 5-week-old Fmr1-KO mice. (A) Hexa-patch recorded cluster of 6 biocytin-stained pyramidal neurons (scale bar 25 μm). Inset top, 8 AP stimulation at 30 Hz with single test pulse 500 ms later, and inset bottom, corresponding EPSPs from monosynaptic connection. (B) Connectivity outline for examples of a recorded WT (2 of 30 possible synaptic connections) and an Fmr1-KO cluster (6 of 30 possible synaptic connections), calculated from a connectivity matrix of all possible synaptic connections for one example cluster (see Supplementary Fig. 1). (C) CP distributions for the clusters of Fmr1-KO ($N = 432$ neurons) and WT neurons ($N = 466$), up to 125 μm apart, were significantly different (Wilcoxon sum rank test, **$P < 0.01$). (D) CP distributions for the clusters of Fmr1-KO ($N = 384$ neurons) and WT neurons ($N = 296$), up to 125 μm apart, were not significantly different from each other (Wilcoxon sum rank test, $P = 0.5$). Individual values listed for both age groups in Supplementary Table 1.

$$\mathrm{SEM} = \sqrt{\frac{\mu \cdot (1-\mu)}{N-1}} \qquad (2)$$

The mean (μ) is calculated per cluster of cells grouped at the specified intersomatic distance bin. For the comparison of CPs along the defined distance ranges, χ^2 test was used. Attributed levels of significance were ($^*P \leqslant 0.05$) and ($^{**}P \leqslant 0.01$). Throughout the text, when referring to CP "n" stands for the number of connections probed. For comparison of CPs across the entire distance range in both WT and KO groups, the Wilcoxon sum rank nonparametric test for distributions was used.

Calculating Kinetic Parameters from Monosynaptic EPSPs
All kinetic parameters were extracted from the average postsynaptic voltage response trace to 30 repetitions of a presynaptic spike train, composed of 8 AP at 30 Hz followed by a recovery test 500 ms later. Each stimulus iteration started 60 s after the end of the previous sweep. The amplitude of the first excitatory postsynaptic potential (EPSP) was calculated from baseline to peak. Rise time and slope of rise were extracted from 20% to 80% rise of the averaged traces.

Fitting the Parameters of the Tsodyks–Markram Model
The dynamics of the short-term depression exhibited by the synapses measured at P12-19 can be captured with the Tsodyks–Markram model (Tsodyks and Markram 1997; Loebel et al. 2009). The model considers a finite amount of resources for a synaptic connection, for example, the available vesicles that are ready to be released, of which a fraction is utilized to evoke the postsynaptic response at the event of an AP. If a subsequent AP arrives before all the utilized resources have recovered, the following postsynaptic response will be smaller. In mathematical terms, the model is represented by the following:

$$\frac{\mathrm{d}x}{\mathrm{d}t} = \frac{1-x}{\tau_{\mathrm{rec}}} - U \cdot x \cdot \delta(t - t_{\mathrm{sp}}), \qquad (3)$$

$$\frac{\mathrm{d}I_{\mathrm{syn}}}{\mathrm{d}t} = -\frac{I_{\mathrm{syn}}}{\tau_{\mathrm{in}}} + A \cdot U \cdot x \cdot \delta(t - t_{\mathrm{sp}}), \qquad (4)$$

where $x(t)$ denotes the fraction of available synaptic resources; U determines the fraction of the resources utilized at each spike and is associated with the release probability of vesicles; and τ_{rec} is the time constant that underlies the recovery of the utilized resources, for example, the characteristic time for an empty release site to be refilled with a new vesicle. $I_{\mathrm{syn}}(t)$ denotes the postsynaptic current that increases, at each spike, in proportion to the amount of utilized resources and decays with a time constant τ_{in}. The proportionality factor, A, represents the absolute synaptic efficacy of the connection. $\delta(t)$ is in the Dirac notation and t_{sp} represent the timing of a spike.

For capturing the short-term facilitating dynamics observed at the P20-36 synaptic connections, we took into consideration the fact that the probability of release is not constant but rather follows the following dynamics (Markram et al. 1998)

$$\frac{\mathrm{d}u}{\mathrm{d}t} = -\frac{u}{\tau_{\mathrm{facil}}} - U \cdot (1-u) \cdot \delta(t - t_{\mathrm{sp}}), \qquad (5)$$

where $u(t)$ denotes the instantaneous release probability that is increased at each spike by $U\dot s(1-u)$ and in between spikes decays exponentially with a characteristic time of τ_{facil}. Substituting $u(t)$ for "U" in equations (3,4) completes the model of short-term facilitation.

Finally, the postsynaptic membrane potential was modeled using a passive membrane mechanism:

$$\tau_{\mathrm{mem}} \frac{\mathrm{d}V}{\mathrm{d}t} = -V + R_{\mathrm{in}} I_{\mathrm{syn}}, \qquad (6)$$

where τ_{mem} is the membrane time constant. For convenience, R_{in}, which represents the input resistance, was absorbed in "A" in the following.

For each synaptic connection, τ_{in} and τ_{mem} were estimated first by fitting the time course of the recovery-test EPSP to the response of the model to a single presynaptic activation (eqs. 4,6):

$$V(t) = \frac{\alpha \tau_{in}}{\tau_{syn} - \tau_{mem}} \cdot \left(e^{-\frac{t}{\tau_{syn}}} - e^{-\frac{t}{\tau_{mem}}} \right), \qquad (7)$$

where α is a scaling factor. Subsequently, the remaining parameters (A, U, τ_{rec}, and τ_{facil} at the P20-36 synaptic connections) were estimated from comparing the experimentally measured amplitudes of the 9 evoked EPSP responses to an analogous set of amplitudes derived analytically from the model (Tsodyks and Markram 1997; Markram et al. (1998)).

Excitatory Network Simulation Model
The network consists of pyramidal neurons, recurrently connected by excitatory short-term depressing synapses (Tsodyks 2005; Holcman and Tsodyks 2006). The electrical activity of the population is described by a single variable z, which represents the average synaptic input to a generic neuron and evolves in time according to

$$\tau \frac{\mathrm{d}z}{\mathrm{d}t} = \left(z_r - z \right) + J \cdot R\left(z \right) + n\left(t \right) + i\left(t \right), \qquad (8)$$

z is measured in arbitrary units and refers to resting baseline activity z_r. Activity of the network changes in time as a result of external afferent inputs $i(t)$, uncorrelated sources of noise $n(t)$ (e.g., spontaneous background firing, channel noise, spontaneous release of neurotransmitter, finite-size network effects, etc.) as well as of the firing rate $R(z)$ of recurrent inputs. In this study, $n(t)$ was modeled as a zero-mean Gaussian-distributed white noise, with variance σ^2. Under the hypotheses of the mean-field approximation (Treves 1993), the recurrent term is approximated by the product between the input–output neuronal response function $R(z)$ and the synaptic efficacy J. The latter proportionally depends on the number of neurons, the probability of pair-wise connectivity and the individual average synaptic conductance. For simplicity, $R(z)$ is defined as a threshold-linear response function: for $z < z_{\mathrm{th}}$, $R(z) = 0$, while for $z \geqslant z_{\mathrm{th}}$, $R(z) = \alpha (z - z_{\mathrm{th}})$.

As individual synaptic responses undergo short-term depression (Tsodyks and Markram 1997), J changes in time with the depression parameter x:

$$J = j \cdot U \cdot x \qquad (9)$$

$$\frac{\mathrm{d}x}{\mathrm{d}t} = \frac{1-x}{\tau_{\mathrm{rec}}} - U \cdot x \cdot R\left(z \right) \qquad (10)$$

Finally, in the lack of external or recurrent inputs, z exponentially decays to rest with a time constant τ (eq. 8), and x exponentially recovers to 1 with a time constant τ_{rec}. Equations (9,10) summarize and directly relate to the short-term depressing dynamics outlined in equation (4) under the same mean-field hypothesis assumed for neuronal response dynamics.

Spontaneously emerging network activity (Fig. 4A–E) was investigated by numerically simulating equations (7–9), setting $i(t) = 0$, while the evoked responses (Fig. 4F) were obtained by applying sinusoidal inputs of the form $i(t) = i_0 + i_1 \sin(2\pi f t)$, with f the frequency of the input oscillations. Under the hypothesis of weak oscillation amplitudes (i.e., $i_1 << i_0$), the steady-state response $z(t)$ was approximately described by $z(t) = z_0 + z_1 \sin(2\pi f t + \varphi)$, with both the modulation amplitude $z_1(t)$ and the phase $\varphi(f)$ varied for varying input frequencies f as in a linear filter.

Due to the onset of facilitating synaptic responses in the older age group (P20-36) tested, the model was extended to include short-term facilitation by replacing the fixed parameter U in equations (9,10) by an activity-dependent variable u (Barak and Tsodyks 2007). Upon activity, u increases until a maximum saturating value of 1 and in the lack of activity u recovers exponentially to its resting value U, with a time constant τ_{facil}:

$$\tau_{\mathrm{facil}} \frac{\mathrm{d}u}{\mathrm{d}t} = U - u + \tau_{\mathrm{facil}} \cdot U \cdot \left(1 - u \right) \cdot R\left(V \right) \qquad (11)$$

Simulation code, developed in MATLAB (The Mathworks, Natick), is available from ModelDB (Hines et al. 2004) at http://senselab.med.yale.edu/modeldb via accession number 140033.

Results

Developmentally Restricted Hyperconnectivity between Medial Prefrontal Cortex Pyramidal Neurons

We used a hexa-patch electrode system to simultaneously record from a cluster of 5 or 6 pyramidal neurons in mPFC living brain slices (Fig. 1A). mPFC slices were made from control (WT) mice and Fmr1-KO mice, a model for the mental retardation and autistic spectrum disorder, Fragile X Syndrome. Pyramidal neurons were classified from both morphological and active electrophysiological characteristics. To test functional connectivity between individual neurons, a train of 8 precisely timed APs was induced in each neuron followed by a recovery pulse 500 ms later, and resultant unitary synaptic responses in the neighboring neurons were measured (Fig. 1A right panel, Supplementary Fig. 1). Direct connections between pairs of layer 5 pyramidal neurons from WT and KO mice were tested at a range of intersomatic distances up to 125 μm in 3D space, within a typical range for estimates of the cortical minicolumn (Buxhoeveden and Casanova 2002). For each group of 5–6 pyramidal neurons in WT and KO slices, the number of direct functional connections was recorded out of a theoretically possible 20–30 connections tested (Fig. 1B). At postnatal days (P) 12–19, the number of connections between pyramidal neurons within the 125-μm range was significantly higher in Fmr1-KO mice than in WT mice (WT: 38 connections from 466 tested, KO: 60 connections from 432 tested, $\chi^2 = 16.8$, $P < 0.01$). To correct for the number of synaptic connections tested, CP was calculated against intersomatic l distance for all neurons. For WT mice, CP was similar across 125-μm cortical distance sampled (Fig. 1C). However, during this early developmental period, Fmr1-KO mice showed a higher CP between 25 and 75 μm and a significantly different distribution of higher connectivity rates compared with WTs (Wilcoxon sum rank test, $^*P < 0.01$, Fig. 1C, Supplementary Table 1). This abnormal connectivity between KO neurons was restricted to the second and third postnatal weeks: at P20–36, the number of connections was not significantly higher in Fmr1-KO than WT neurons (WT: 20 connections from 296 tested, KO: 29 connections from 384 tested, $\chi^2 = 0.16$, $P = 0.7$). Furthermore, the corresponding CP did not differ significantly between WT and KO groups at this later developmental stage (Wilcoxon sum rank test, $P = 0.50$, Fig. 1D, Supplementary Table 1).

The mPFC is a highly interconnected region with a higher proportion of reciprocally connected neurons compared with sensory neocortex (Mason et al. 1991; Thomson et al. 1993; Wang et al. 2006). A high level of reciprocal feedback between neurons is proposed to underlie recurrent networks in the cortex (Markram 1997). Therefore, we further investigated the proportion of bidirectional (reciprocal) connections within the directly connected neurons. Between P12–19, 4 of the 38 direct WT synaptic connections were reciprocal (10.5%). In Fmr1-KO mice, reciprocity occurred in 10 of the 60 identified synaptic connections (16.7%), which was not statistically different from WTs ($\chi^2 = 0.7$, $P = 0.4$). At P20–36, no significant difference in reciprocity was observed between WT and KO neurons ($\chi^2 = 0.1$, $P = 0.8$), with 4 of 20 WT (20%) and 5 of 29 KO (17.2%) reciprocal connections, respectively.

Thus, layer 5 pyramidal neurons exhibit transient hyperconnectivity during an early postnatal period within the mPFC in Fmr1-KO mice. No significant net increase in recurrent connectivity was observed in KO mice within layer 5 mPFC at any developmental stage tested.

Synaptic Maturation of mPFC Layer 5 Pyramidal Circuitry

Integration and processing of information within neuronal networks in the brain is influenced by synaptic strength and the dynamic ability to alter the efficacy of connections (Nelson and Turrigiano 2008). We investigated whether the kinetic and dynamic properties of excitatory synapses between layer 5 pyramidal neuron differed between KO and WT mice during prefrontal cortex circuit development (Fig. 2). At P12–19, we found that the majority of unitary connections between layer 5
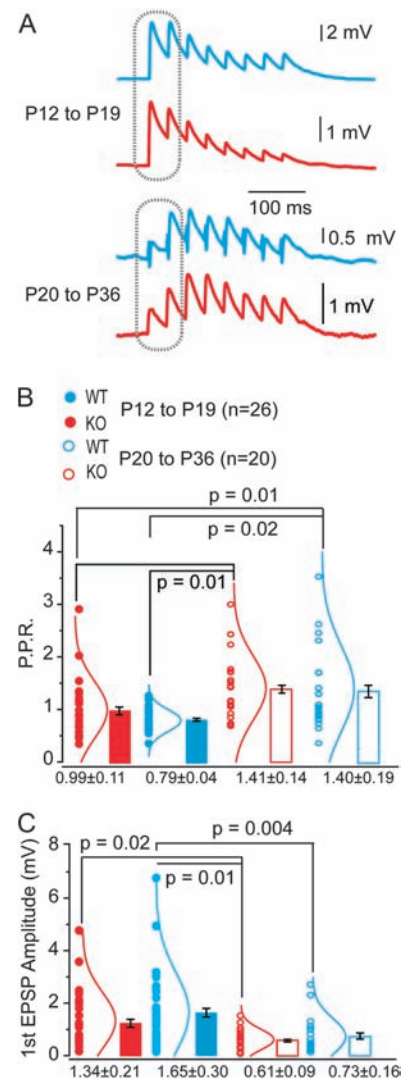
Figure 2. Synaptic maturation and dynamics of WT and Fmr1-KO connections during development. (A) Example EPSP traces of typical responses to AP trains in WT (blue) or KO neurons (red) at P12–19 (above) and P20–36 (below). (B) Paired-pulse ratios, measured at responses indicated on traces in A, are significantly increased in the older age groups for both WT and KO. *P values indicated, Fisher's analysis of variance (ANOVA). No significant difference exists between WT and KO at either age group. Mean ± SEM shown. Individual data points (circles) and the corresponding normal distribution curves shown by each bar. (C) Amplitude of first EPSP in evoked train is significantly reduced in older age groups (P20–36) compared with younger (P12–19) for both WT and KO neurons. *P values indicated, Fisher's ANOVA. Mean ± SEM shown. Individual data points (circles) and the corresponding normal distribution curves shown by each bar.

pyramidal neurons showed depressing responses to a train of APs (WT: 24 of 26 tested; KO: 23 of 26 tested, Fig. 2A) similar to synaptic depression between layer 5 neurons in sensory and frontal cortex of rat and ferret (Wang et al. 2006; Rinaldi et al. 2008; Berger et al. 2009). At P12–19, paired-pulse responses (PPRs) showed a tendency to depress more compared with P20–36 PPR ranges and were not significantly different between WT or Fmr1-KO neurons (WT: 0.99 ± 0.11, KO: 0.79 ± 0.04, Fig. 2B). In contrast, the majority of monosynaptic connections in the older age group were facilitating, with PPR responses significantly larger than those at P12–19 for both KO and WT (WT: 1.41 ± 0.14, KO: 1.40 ± 0.19, * P < 0.05 for both genotype groups, Fig. 2A,B).

Unitary EPSPs of KO and WT synapses did not differ in amplitude or total rise time within each age group (Fig. 2C and Table 1). However, synapses matured at a similar rate, with a significant developmental decrease in synaptic amplitude occurring in both WT and KO neurons (WT: 1.65 ± 0.3 to 0.61 ± 0.09 mV *P < 0.01, KO: 1.34 ± 0.21 to 0.73 ± 0.16 mV *P = 0.02, Fig. 2C).

Therefore, despite early hyperconnectivity between synapses in Fmr1-KO mice, the subsequent maturation of monosynaptic responses between layer 5 mPFC neurons exhibited normal developmental changes in both synapse amplitude and the appearance of synapse facilitation up to 5 weeks postnatal age.

Table 1
Kinetic and dynamic properties of unitary EPSPs of WT and Fmr1-KO synapses

P12—P19

EPSP parameter	Genotype		P value
	WT (N = 26)	KO (N = 26)	
First EPSP amplitude (mV)	1.6 ± 0.3	1.3 ± 0.2	P = 0.39
Rise time (ms)	1.3 ± 0.1	1.4 ± 0.1	P = 0.59
Slope of rise (mV/ms)	0.77 ± 0.15	0.62 ± 0.09	P = 0.40

Model parameter	Genotype		P value
	WT (N = 24)	KO (N = 23)	
Absolute synaptic efficacy (mV)	7.1 ± 1.0	5.8 ± 0.9	P = 0.44
Probability of release (%)	0.28 ± 0.03	0.28 ± 0.03	P = 0.92
$\tau_{recovery}$ (ms)	547 ± 46	745 ± 82	*P < 0.05
$\tau_{inactivation}$ (ms)	1.8 ± 0.1	1.8 ± 0.2	P = 0.99
$\tau_{membrane}$ (ms)	21 ± 2	21 ± 2	P = 0.76

P20–P36

EPSP parameter	Genotype		P value
	WT (N = 14)	KO (N = 14)	
First EPSP amplitude (mV)	0.73 ± 0.09 (N = 20)	0.61 ± 0.16 (N = 20)	P = 0.81
Rise time (ms)	1.9 ± 0.2	1.9 ± 0.1	P = 0.89
Slope of rise (mV/ms)	0.68 ± 0.53	0.40 ± 0.10	P = 0.26

Model parameter	Genotype		P value
	WT (N = 11)	KO (N = 19)	
Absolute synaptic efficacy (mV)	2.4 ± 0.9	3.2 ± 0.9	P = 0.57
Probability of release (%)	0.19 ± 0.03	0.20 ± 0.03	P = 0.62
$\tau_{recovery}$ (ms)	511 ± 79	373 ± 54	P = 0.15
$\tau_{inactivation}$ (ms)	2.1 ± 0.3	2.3 ± 0.3	P = 0.58
$\tau_{membrane}$ (ms)	24 ± 2	27 ± 3	P = 0.44
$\tau_{facilitation}$ (ms)	80 ± 19	120 ± 25	P = 0.26

Note: Measurements for WT P12–19 (n = 26), Fmr1-KO P12–19 (n = 26), WT P20–36 (n = 14), and Fmr1-KO P20–36 (n = 14) synapses recorded from unitary excitatory connections and determined by Tsodyks-Markram model.
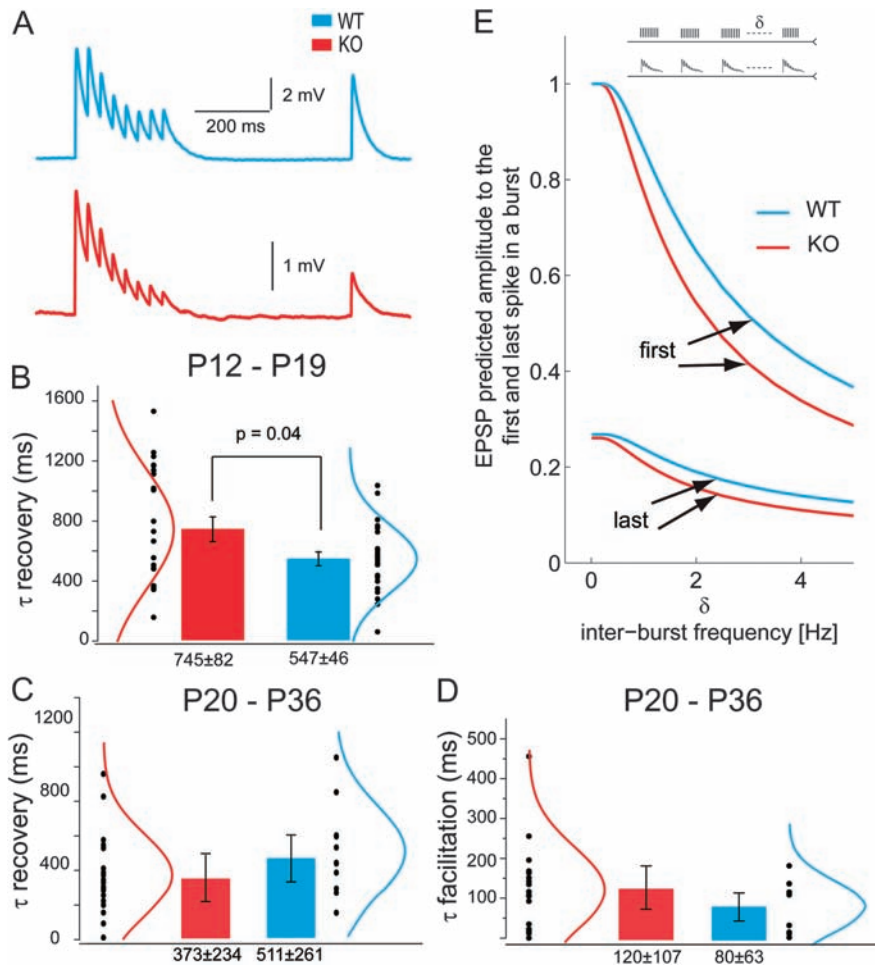
Slow Synaptic Recovery Following Short-Term Depression in Fmr1-KO Neurons

Synaptic transmission is a dynamic process with specific input pathways exhibiting facilitation or depression over a timescale of hundreds of milliseconds to seconds. Depressing synapses act as low-pass filters by attenuating high-frequency presynaptic firing of inputs (Izhikevich et al. 2003). Given the longer duration of UP-state excitability in developing somatosensory cortex (Gibson et al. 2008) and increased cellular excitability in amygdala (Olmos-Serrano et al. 2010) of Fmr1-KO mice, we further investigated whether the short-term dynamics and repetitive activation of synaptic responses were significantly altered in KO mPFC synapses. The dynamics of cortical synaptic responses are due to interplay between release probability, synaptic efficacy, and the time constant of the synapse to recover from depression. Using the Tsodyks-Markram model, we fitted the trains of EPSP traces (Tsodyks and Markram 1997) and explored the mechanisms underlying the short-term dynamics of synaptic transmission to a brief 30-Hz train of stimuli for both WT and KO synapses at P12-19 and P20–36 (for model parameters, see Materials and Methods, Fig. 3A). Synaptic efficacy and release probability were not significantly different between WT and KO synapses at P12-19, indicating similar synaptic strength (Table 1). However, we found a significantly slower recovery (τ_{rec}) from short-term depression in KO compared with WT mice in the P12-19 group (KO: 745 ± 82 ms, WT: 547 ± 46 ms, * P < 0.05, Fig. 3B). This delay in recovery was a dynamic property of the synapses rather than a baseline feature, since the slopes of the EPSP rising and falling phases for the recovery pulse (quantified by τ_{in} and τ_{mem}) were not different from those measured at WT synapses (see Table 1). No significant differences in the recovery from depression or time constants for facilitation in the older age group, P20–36, were observed between WT and KO neurons (Fig. 3C,D and Table 1; τ_{rec} KO: 373 ± 234, WT: 511 ± 261 ms; τ_{facil} KO: 120 ± 107, WT: 80 ± 63 ms).

Using the best-fit model parameters identified in the experiments, computer simulations predicted that repeated stimulation of a depressing synapse would give rise to weaker subsequent synaptic responses in the KO cortex, compared with WT within the P12-19 range. For differing interstimulation times intervals δ at low frequencies between 0 and 4 Hz, we found that the EPSP amplitudes of the first and last responses following repetitive bursts of presynaptic APs were diminished in KO synaptic connections (Fig. 3E). Thus, layer 5 synaptic connections between pyramidal neurons are temporally attenuated in Fmr1-KO mice during the second and third postnatal weeks (P12-19). Slower recovery from depression impedes the ability of the synapse to act as a low-pass filter during repetitive synaptic network activation. This will have significant implications for information processing in developing mPFC during activation over a period of a few seconds, at a timescale relevant for functional processing during attention and working memory processes in frontal cortex (Miller 2000).

Consequences of Hyperconnectivity and Slow Synaptic Recovery Upon Early Excitatory Network Development

To investigate the implication of hyperconnectivity and slower temporal synaptic dynamics in the young age group, we manipulated these parameters in a network model of excitatory cortical neurons (Tsodyks 2005; Holcman and Tsodyks 2006).

Figure 3. Delayed recovery of EPSPs following short-term depression in Fmr1-KO synapses. (*A*) Example EPSP traces from evoked AP trains from WT (blue) and KO (red) synaptic connections used for extracting the 5 synaptic dynamic parameters with the T-M model. See Materials and Methods for model fitting details. (*B*) The recovery time constant from depression, τ_{rec}, is significantly delayed in Fmr1-KO than WT synapses *P < 0.04. Mean ± SEM shown. Individual data points (black circles) and the corresponding normal distribution curves shown by each bar. No significant differences in other dynamic parameters or in absolute synaptic efficacy were observed. (*C*) No significant difference exists in the recovery time constant from depression τ_{rec}, between KO and WT synapses. Mean ± SEM shown. (*D*) Time constant of synaptic facilitation, τ_{facil}, is measured only in older synapses and does not differ between KO and WT groups. Mean ± SEM shown. Individual data points (black circles) and the corresponding normal distribution curves shown by each bar. (*E*) Smaller EPSP amplitudes in response to first and last spike in the 8 AP train at 30 Hz for WT and KO synapse simulation, repeatedly stimulated at intervals (δ) of 0–5 Hz, as predicted by the model (eqs. 3,4).

This approach enabled us to identify the individual contributions of connectivity and recovery time constants to the readout activity of the network. Under baseline conditions, the network displayed a dynamic range of activity, characterized by high and low states of excitation and short periods of synchronous firing (Fig. 4*A*). Increasing the connectivity in accordance with experimental values (see Fig. 1*C*) saw a marked transition to higher excitation but abolished the dynamic network states (Fig. 4*B*). Alternatively, increasing the time constants of recovery from depression, using WT and KO synaptic values obtained for P12-19 in Figure 3, shifted the network to a lower activation state with short bursts of synchronous firing but absence of sustained high firing rates (Fig. 4*C*). However, co-occurrence of high connectivity with slower synaptic recovery times, simulating the experimental findings from the Fmr1-KO synapses, shifted the network back to its original state, in which it exhibits both high and low states of activation (Fig. 4*D*). Thus, slowed temporal processing enabled the hyperconnected excitatory network to operate within a dynamic range of spontaneous network activity (Fig. 4*E*).

In addition to spontaneous network dynamics, we further tested the activation of the network over a physiological range of frequencies. The evoked network response revealed resonating filtering properties at a low frequency range (Fig. 4*F*). This response could be enhanced or attenuated by increasing the network connectivity or by slowing down the time constant of recovery from depression, respectively. Co-occurrence of high connectivity with slower recovery times, as in the Fmr1-KO simulated network (Fig. 4*C*) resulted in a decreased responsiveness to low frequency stimulation of 9% compared with WT simulated network (Normalized peak gain WT 1.31, KO 1.195, 0.5-0.6 Hz range). Thus, slower recovery from depression at the synapse (Fig. 3*C*) impaired the ability of the entire network to respond to repeated stimuli at low activation frequencies. The ability of the synaptic network to operate as a high-pass temporal filter was not affected, in line with the lack of difference in synaptic efficacy observed at WT and KO synapses (Table 1). This will have significant implications for information processing in the developing mPFC during attentional and repetitive working memory procedures.
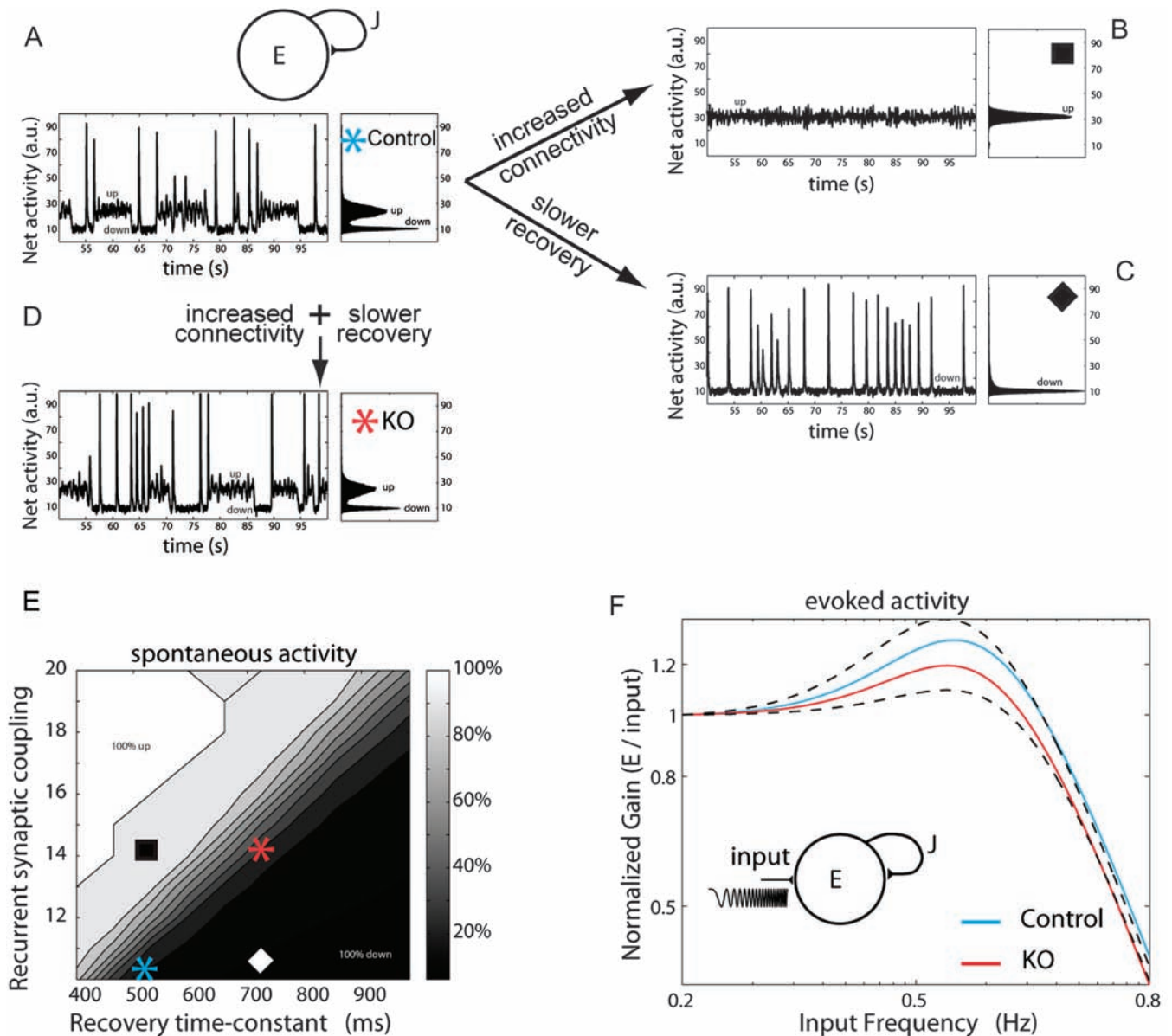
Figure 4. Slower time constants counterbalance hyperconnectivity in a developing network model of Fmr1-KO cortex. (*A*) Above, schematic of the recurrent network model that includes connectivity strength J and synaptic connections that exhibit short-term depression (see Materials and Methods). Below, the WT network displays a dynamic range of activity states for periods of a few seconds with transient high discharges of synchronous firing (left). Histogram of mean network activity illustrates bistable network state interspersed with transient high-firing synchrony (right). (*B–D*) Increased connectivity or slower tau recovery constants from depression significantly alter the network activity. Co-occurrence of increased connectivity and slow tau recovery, simulating experimental data from KO synapses, rescue the dynamic transitions of the network. (*E*) Map of spontaneous activity revealing relative changes in recurrent synaptic connections against recovery time constant after depression for 4 different network states, as shown in *A–D*. (*F*) Evoked stimulation at a range of physiological rhythm frequencies reveals lower gain entrainment of KO synaptic networks between 0.5 and 0.6 Hz range.

Developmental Maturation of Synaptic mPFC Network

Our experimental data revealed that by 3–5 weeks postnatal development, synapses in both WT and KO mice exhibited significantly decreased synapse amplitudes and a switch from depressing to facilitating synaptic dynamics (Figs 2 and 3). We therefore further investigated how these normal maturational changes in synapse properties affected dynamic network activity in our model. Increasing the level of synaptic facilitation to mimic developmental maturation pushed the network into a prolonged upstate mode and abolished the dynamic transitions between high and low activity states (Fig. 5*A,D*). Developmental decreases in synaptic efficacy (Table 1), reflecting in part a reduction in EPSP amplitude

(Fig. 2*C*), significantly affected the balance of activity, pushing the network into a downstate with considerably shortened periods of firing (Fig. 5*B*). However, a combination of decreased synapse efficacy and the onset of facilitation could counteract both states of reduced network transitions and enable the mature network to operate over a dynamic range of activity (Fig. 5*C,E*).

Discussion

Our findings reveal a clear local hyperconnectivity during early mPFC network development and confirm neurocognitive theory predictions at the synaptic level in a mouse model for mental
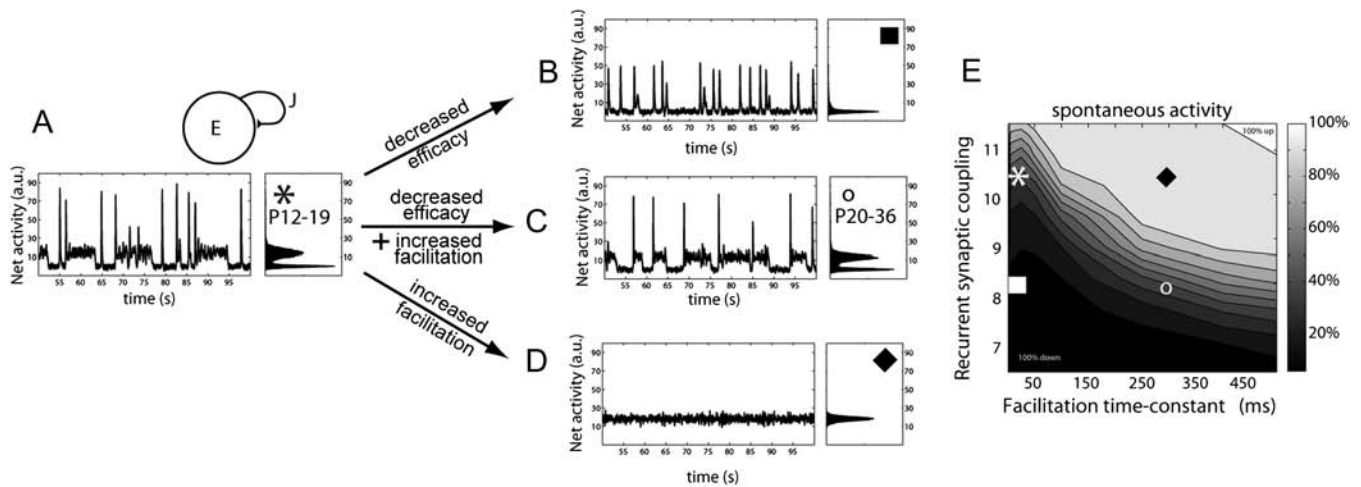
Figure 5. Decreased synaptic efficacy during maturation counterbalances the appearance of short-term facilitation, in a network model of young adult cortex. (*A*) Above, schematic of the recurrent network model that includes connectivity strength J and synaptic connections that exhibit both short-term depression and facilitation (see Materials and Methods). Below, the adult network displays a dynamic range of activity states for periods of a few seconds with transient high discharges of synchronous firing (left). Histogram of mean network activity illustrates bistable network state interspersed with transient high-firing synchrony (right). (*B–D*) Decreased efficacy of synaptic transmission or increased facilitation significantly alters the network activity. Co-occurrence of decreased efficacy and increased facilitation in adult networks simulating experimental data from synapses in young adult animals, rescue the dynamic transitions of the network. (*E*) Map of spontaneous activity revealing relative changes in recurrent synaptic connections against facilitation time constant for 4 different networks, as shown in *A–D*. Compare to panel *E* of Figure 4 and note the smaller values for recurrent synaptic coupling.

retardation and autism disorder. In addition, we found that these depressing synaptic connections exhibit slower temporal dynamics of recovery. Slower temporal processing rescues the nonfluctuating rigid level of activity in a hyperconnected network and is necessary to enable developing excitatory cortical networks to maintain a dynamic range of activity. However, it predicts that, as a side effect, the network will exhibit a reduced responsiveness to repetitive low-frequency stimuli. Finally, our data reveal that the developmental stage is critical to reveal impairments in Fmr1-KO synaptic networks: both hyperconnectivity and slow synapse dynamics are restricted to a time window of 2–3 weeks postnatal development, before the restoration of a normal pattern of synaptic maturation at 3–5 weeks age.

Abnormalities in neuronal connectivity of the brain have been defined at many different levels from functional imaging to synapse pathology in NDDs (Kaufmann and Moser 2000; Belmonte et al. 2004; Belmonte and Bourgeron 2006; Dinstein et al. 2011). In the Fmr1-KO mouse model, altered density and length of spine protrusions occurs in superficial and deep layers of the neocortex (Nimchinsky et al. 2001; Irwin et al. 2002; Galvez and Greenough 2005; Meredith et al. 2007). This increase likely arises from more immature filopodial protrusions (Cruz-Martin et al. 2010). However, it is not clear if increased spine protrusions result in altered dynamics and connectivity of excitatory synaptic transmission. Our findings show enhanced local connectivity between layer 5 pyramidal neurons between P12 and 19, which correlates with an increase in protrusion density and may arise from alterations in spine formation and pruning, proposed to occur in Fragile X syndrome (Bagni and Greenough 2005). Within neuronal networks, hyperconnected synapses will affect the level and stability of recurrent excitation—a key feature proposed to mediate working memory and attention in prefrontal cortex (Miller et al. 1996; Miller 2000). Thus, enhanced local excitation in hyperconnected mPFC networks provides strong

evidence for early onset alterations in synaptic networks underlying cognitive deficits in mental retardation and autism.

There is increasing evidence of developmentally regulated time windows in the Fmr1-KO mouse for Fragile X syndrome, within which dendritic spine morphology, synaptic transmission, and plasticity are significantly altered (Harlow et al. 2010; Meredith and Mansvelder 2010; Portera-Cailliau 2011). Our data show significant hyperconnectivity and slow synapse dynamics in layer 5 neurons of mPFC at 2–3 weeks but not 3–5 weeks postnatal development. This restricted period for changes in synaptic function reflects the changing pattern for morphological spine differences in layer 5 pyramidal neurons in the neocortex of Fmr1-KO mice, where longer spines are found at P7 and P14 but not P30 (Nimchinsky et al. 2001). The immature spine phenotype of these KO neurons, however, returns by young adulthood (P73–76) (Galvez and Greenough 2005). Based on these observations, we speculate that the synaptic hyperconnectivity phenotype could return in fully mature mPFC neurons of Fmr1-KO mice and give rise to a hyperconnected excitatory network.

The mPFC is a key neocortical region underlying working memory (Goldman-Rakic 1995; Mongillo et al. 2008). Persistent, reverberating neuronal activity has been proposed as a mechanism to underlie working memory (Miller et al. 1996). In rodent data, monosynaptic connections between layer 5 pyramidal neurons were found to exhibit short-term depression to a train of responses in juvenile rats (Hempel et al. 2000; Rinaldi et al. 2008; Berger et al. 2009), which would work against persistent activation as an underlying mechanism. However, these same synapses exhibit short-term facilitation in young adult ferrets and rats (Wang et al. 2006, 2008). Our data reveal that synapses between layer 5 pyramidal neurons undergo a developmental transition, displaying short-term depression in juvenile mouse mPFC (P12–19) and initial synaptic facilitation in later stages of mPFC maturity (P20–36). This developmental increase in synaptic facilitation increased the persistent excitability of the network in our

cortical model, supporting the idea of its role underlying working memory in the mature brain. To preserve the dynamic range of activity, it was necessary to decrease the synaptic efficacy of the network overall, in line with a downregulation of synaptic responses after a critical period of heightened synapse remodeling and plasticity during early stages of postnatal development.

Timing of synaptic inputs is critical for refinement of synaptic strength and synchrony of neuronal output during development (Sjostrom and Nelson 2002). Synaptic and neuronal membrane time constants of immature neurons are slower and longer (Oswald and Reyes 2008; Feldmeyer and Radnikow 2009). Our data reveal an impaired ability of the synapse to recover following a short train of pulses in the Fmr1-KO mouse, consistent with slower synaptic membrane properties of immature spine and filopodial protrusions in early cortical developmental stages. In NDDs, both input-specific synaptic plasticity and synchronous network activity are abnormal in frontal cortex (Uhlhaas and Singer 2006; Meredith et al. 2007). Our network simulations demonstrate the net effects of altered connectivity or slowed temporal dynamics upon excitatory synaptic network activity. A dynamic range of activity can only be maintained by counterbalancing synaptic hyperconnectivity with slowed recovery from synaptic depression. On a milliseconds time-scale, dynamic properties of the synapse regulate information processing at specific frequencies through a network (Izhikevich et al. 2003). Fmr1-KO synapses show similar synaptic depression to a burst of stimuli at beta–gamma frequency range (30 Hz) as WT synapses. However, the impaired ability of KO synapses to directly recover from this depression impedes their subsequent responsiveness and therefore signal integration over slower frequencies of less than a few hertz. Central coherence theory of autism proposes that impairments in the integration of complex information processing in the brain underlie the inability to construct higher level meaning in aspects of cognition in autistic disorders (Happe and Frith 1996). During an attention task, significant changes in electroencephalography (EEG) delta activity bands have been linked to alterations in the subject's internal processing during mental calculations (Harmony et al. 1996). EEG studies in juveniles with autism spectrum disorder reveal decreases in delta (1.5–3.5 Hz) activity across frontal cortex and decreased long-range coherence across the cortex (Coben et al. 2008). It was not known what synaptic mechanisms could mediate this altered integration of information processing in prefrontal cortex: our data propose that slowed temporal dynamics of excitatory synapses co-occur with hyperconnective networks to maintain dynamic activity states but at the cost of impaired processing during low-frequency stimulation.

Thus, our data provide a synaptic model for functional hyperconnectivity in local neuronal networks in early stages of NDDs. Furthermore, hyperconnectivity is accompanied by significantly slower processing at the millisecond timescale in excitatory synapses. Disruption in the timing of synaptic signaling has a significant impact upon later neuronal development and network function in autistic disorders (Zoghbi 2003). Alterations in synapse timing at an early time window of development, when synaptic connectivity and plasticity are believed to be heightened (Stern et al. 2001; Calabrese et al. 2006) will likely have long-lasting implications for network

activity. Therefore, co-occurrence of synaptic delay and increased neuronal coupling at this early developmental stage of mPFC may underlie deficits in frontal processing in the brain in NDDs of autism and mental retardation.

Supplementary Material

Funding

Notes

Conflict of Interest: None declared.

References

Bagni C, Greenough WT. 2005. From mRNP trafficking to spine dysmorphogenesis: the roots of fragile X syndrome. Nat Rev Neurosci. 6:376–387.

Bakker CE, et al. 1994. Fmr1 knockout mice: a model study to fragile X mental retardation. Cell. 78(1):23–33.

Barak O, Tsodyks M. 2007. Persistent activity in neural networks with dynamic synapses. PLoS Comput Biol. 3:e35.

Belmonte MK, Allen G, Beckel-Mitchener A, Boulanger LM, Carper RA, Webb SJ. 2004. Autism and abnormal development of brain connectivity. J Neurosci. 24:9228–9231.

Belmonte MK, Bourgeron T. 2006. Fragile X syndrome and autism at the intersection of genetic and neural networks. Nat Neurosci. 9:1221–1225.

Berger TK, Perin R, Silberberg G, Markram H. 2009. Frequency-dependent disynaptic inhibition in the pyramidal network: a ubiquitous pathway in the developing rat neocortex. J Physiol. 587:5411–5425.

Buxhoeveden DP, Casanova MF. 2002. The minicolumn hypothesis in neuroscience. Brain. 125:935–951.

Calabrese B, Wilson MS, Halpain S. 2006. Development and regulation of dendritic spine synapses. Physiology. 21:38–47.

Chapleau CA, Calfa GD, Lane MC, Albertson AJ, Larimore JL, Kudo S, Armstrong DL, Percy AK, Pozzo-Miller L. 2009. Dendritic spine pathologies in hippocampal pyramidal neurons from Rett syndrome brain and after expression of Rett-associated MECP2 mutations. Neurobiol Dis. 35:219–233.

Coben R, Clarke AR, Hudspeth W, Barry RJ. 2008. EEG power and coherence in autistic spectrum disorder. Clin Neurophysiol. 119:1002–1009.

Cruz-Martin A, Crespo M, Portera-Cailliau C. 2010. Delayed stabilization of dendritic spines in fragile X mice. J Neurosci. 30:7793–7803.

Dinstein I, Pierce K, Eyler L, Solso S, Malach R, Behrmann M, Courchesne E. 2011. Disrupted neural synchronization in toddlers with autism. Neuron. 70:1218–1225.

Ewen JB, Shapiro BK. 2005. Disorders of attention or learning in neurodevelopmental disorders. Semin Pediatr Neurol. 12:229–241.

Feldmeyer D, Radnikow G. 2009. Developmental alterations in the functional properties of excitatory neocortical synapses. J Physiol. 587:1889–1896.

Fuster JM. 2001. The prefrontal cortex—an update: time is of the essence. Neuron. 30:319-333.

Galvez R, Greenough WT. 2005. Sequence of abnormal dendritic spine development in primary somatosensory cortex of a mouse model of the fragile X mental retardation syndrome. Am J Med Genet A. 135:155-160.

Geschwind DH, Levitt P. 2007. Autism spectrum disorders: developmental disconnection syndromes. Curr Opin Neurobiol. 17:103-111.

Gibson JR, Bartley AF, Hays SA, Huber KM. 2008. Imbalance of neocortical excitation and inhibition and altered UP states reflect network hyperexcitability in the mouse model of fragile X syndrome. J Neurophysiol. 100(5):2615-2626.

Gill TM, Sarter M, Givens B. 2000. Sustained visual attention performance-associated prefrontal neuronal activity: evidence for cholinergic modulation. J Neurosci. 20:4745-4757.

Goldman-Rakic PS. 1995. Architecture of the prefrontal cortex and the central executive. Ann N Y Acad Sci. 769:71-84.

Happe F, Frith U. 1996. The neuropsychology of autism. Brain. 119(Pt 4):1377-1400.

Harlow EG, Till SM, Russell TA, Wijetunge LS, Kind P, Contractor A. 2010. Critical period plasticity is disrupted in the barrel cortex of FMR1 knockout mice. Neuron. 65:385-398.

Harmony T, Fernández T, Silva J, Bernal J, Díaz-Comas L, Reyes A, Marosi E, Rodríguez M, Rodríguez M. 1996. EEG delta activity: an indicator of attention to internal processing during performance of mental tasks. Int J Psychophysiol. 24:161-171.

Hempel CM, Hartman KH, Wang XJ, Turrigiano GG, Nelson SB. 2000. Multiple forms of short-term plasticity at excitatory synapses in rat medial prefrontal cortex. J Neurophysiol. 83:3031-3041.

Hines ML, Morse T, Migliore M, Carnevale NT, Shepherd GM. 2004. ModelDB : a database to support computational neuroscience. J Comput Neurosci. 17:7-11.

Holcman D, Tsodyks M. 2006. The emergence of Up and Down states in cortical networks. PLoS Comput Biol. 2:e23.

Horikawa K, Armstrong WE. 1988. A versatile means of intracellular labeling : injection of biocytin and its detection with avidin conjugates. J Neurosci Methods. 25:1-11.

Huttenlocher PR. 1990. Morphometric study of human cerebral cortex development. Neuropsychologia. 28:517-527.

Irwin SA, Idupulapati M, Gilbert ME, Harris JB, Chakravarti AB, Rogers EJ, Crisostomo RA, Larsen BP, Mehta A, Alcantara CJ, et al. 2002. Dendritic spine and dendritic field characteristics of layer V pyramidal neurons in the visual cortex of fragile-X knockout mice. Am J Med Genet. 111:140-146.

Izhikevich EM, Desai NS, Walcott EC, Hoppensteadt FC. 2003. Bursts as a unit of neural information: selective communication via resonance. Trends Neurosci. 26:161-167.

Just MA, Cherkassky VL, Keller TA, Minshew NJ. 2004. Cortical activation and synchronization during sentence comprehension in high-functioning autism: evidence of underconnectivity. Brain. 127:1811-1821.

Kaufmann WE, Moser HW. 2000. Dendritic anomalies in disorders associated with mental retardation. Cereb Cortex. 10:981-991.

Loebel A, Silberberg G, Helbig D, Markram H, Tsodyks M, Richardson MJ. 2009. Multiquantal release underlies the distribution of synaptic efficacies in the neocortex. Front Comput Neurosci. 3:27.

Markram H. 1997. A network of tufted layer 5 pyramidal neurons. Cereb Cortex. 7:523-533.

Markram H, Wang Y, Tsodyks M. 1998. Differential signaling via the same axon of neocortical pyramidal neurons. Proc Natl Acad Sci U S A. 95:5323-5328.

Mason A, Nicoll A, Stratford K. 1991. Synaptic transmission between individual pyramidal neurons of the rat visual cortex in vitro. J Neurosci. 11:72-84.

Meredith RM, Holmgren CD, Weidum M, Burnashev N, Mansvelder HD. 2007. Increased threshold for spike-timing-dependent plasticity is caused by unreliable calcium signaling in mice lacking fragile X gene FMR1. Neuron. 54:627-638.

Meredith RM, Mansvelder H. 2010. STDP and mental retardation: dysregulation of dendritic excitability in Fragile X syndrome. Front Synaptic Neurosci. 2:10.

Miller EK. 2000. The prefontral cortex and cognitive control. Nat Rev Neurosci. 1:59-65.

Miller EK, Erickson CA, Desimone R. 1996. Neural mechanisms of visual working memory in prefrontal cortex of the macaque. J Neurosci. 16:5154-5167.

Mongillo G, Barak O, Tsodyks M. 2008. Synaptic theory of working memory. Science. 319:1543-1546.

Nelson SB, Turrigiano GG. 2008. Strength through diversity. Neuron. 60:477-482.

Nimchinsky EA, Oberlander AM, Svoboda K. 2001. Abnormal development of dendritic spines in FMR1 knock-out mice. J Neurosci. 21:5139-5146.

Olmos-Serrano JL, Paluszkiewicz SM, Martin BS, Kaufmann WE, Corbin JG, Huntsman MM. 2010. Defective GABAergic neurotransmission and pharmacological rescue of neuronal hyperexcitability in the amygdala in a mouse model of fragile X syndrome. J Neurosci. 30:9929-9938.

Oswald AM, Reyes AD. 2008. Maturation of intrinsic and synaptic properties of layer 2/3 pyramidal neurons in mouse auditory cortex. J Neurophysiol. 99:2998-3008.

Portera-Cailliau C. 2011. Which Comes first in Fragile X syndrome, dendritic spine dysgenesis or defects in circuit plasticity? Neuroscientist. [Epub ahead of print].

Purpura DP. 1974. Dendritic spine "dysgenesis" and mental retardation. Science. 186:1126-1128.

Rinaldi T, Perrodin C, Markram H. 2008. Hyper-connectivity and hyper-plasticity in the medial prefrontal cortex in the valproic Acid animal model of autism. Front Neural Circuits. 2:4.

Silverman JL, Yang M, Lord C, Crawley JN. 2010. Behavioural phenotyping assays for mouse models of autism. Nat Rev Neurosci. 11:490-502.

Sjostrom PJ, Nelson SB. 2002. Spike timing, calcium signals and synaptic plasticity. Curr Opin Neurobiol. 12:305-314.

Stern EA, Maravall M, Svoboda K. 2001. Rapid development and plasticity of layer 2/3 maps in rat barrel cortex in vivo. Neuron. 31:305-315.

Thomson AM, Deuchars J, West DC. 1993. Large, deep layer pyramid-pyramid single axon EPSPs in slices of rat motor cortex display paired pulse and frequency-dependent depression, mediated pre-synaptically and self-facilitation, mediated postsynaptically. J Neurophysiol. 70:2354-2369.

Treves A. 1993. Mean-field analysis of neuronal spike dynamics. Network: Comput Neural Syst. 4:259-284.

Tsodyks M. 2005. Attractor neural networks and spatial maps in hippocampus. Neuron. 48:168-169.

Tsodyks MV, Markram H. 1997. The neural code between neocortical pyramidal neurons depends on neurotransmitter release probability. Proc Natl Acad Sci U S A. 94:719-723.

Uhlhaas PJ, Singer W. 2006. Neural synchrony in brain disorders: relevance for cognitive dysfunctions and pathophysiology. Neuron. 52(1):155-168.

Wang H, Stradtman GG, Wang X-J, Gao W-J. 2008. A specialized NMDA receptor function in layer 5 recurrent microcircuitry of the adult rat prefrontal cortex. Proc Natl Acad Sci. 105:16791-16796.

Wang Y, Markram H, Goodman PH, Berger TK, Ma J, Goldman-Rakic PS. 2006. Heterogeneity in the pyramidal network of the medial prefrontal cortex. Nat Neurosci. 9:534-542.

Zoghbi HY. 2003. Postnatal neurodevelopmental disorders: meeting at the synapse? Science. 302:826-830.